Molecular Biology of the Cell
Vol. 12, 297–308, February 2001

Genome-wide Responses to Mitochondrial Dysfunction[V]

Charles B. Epstein,*† James A. Waddle,* Walker Hale IV,* Varshal Davé,*‡ Janet Thornton,* Timothy L. Macatee,* Harold R. Garner,§ and Ronald A. Butow*‖

*Department of Molecular Biology, and §McDermott Center for Human Growth and Development and Center for Biomedical Inventions, University of Texas Southwestern Medical Center, Dallas, Texas 75390-9148

Submitted August 9, 2000; Revised November 13, 2000; Accepted November 16, 2000
Monitoring Editor: Thomas D. Fox

Mitochondrial dysfunction can lead to diverse cellular and organismal responses. We used DNA microarrays to characterize the transcriptional responses to different mitochondrial perturbations in *Saccharomyces cerevisiae*. We examined respiratory-deficient petite cells and respiratory-competent wild-type cells treated with the inhibitors of oxidative phosphorylation antimycin, carbonyl cyanide *m*-chlorophenylhydrazone, or oligomycin. We show that respiratory deficiency, but not inhibition of mitochondrial ATP synthesis per se, induces a suite of genes associated with both peroxisomal activities and metabolite-restoration (anaplerotic) pathways that would mitigate the loss of a complete tricarboxylic acid cycle. The array data suggested, and direct microscopic observation of cells expressing a derivative of green fluorescent protein with a peroxisomal matrix-targeting signal confirmed, that respiratory deficiency dramatically induces peroxisome biogenesis. Transcript profiling of cells harboring null alleles of *RTG1, RTG2,* or *RTG3*, genes known to control signaling from mitochondria to the nucleus, suggests that there are multiple pathways of cross-talk between these organelles in yeast.

INTRODUCTION

Mitochondria are essential organelles whose primary function is the synthesis of ATP by oxidative phosphorylation. Mitochondria are also the site of many important metabolic and biosynthetic reactions, such as the tricarboxylic acid (TCA) cycle, amino acid, and heme biosynthesis. The biogenesis of mitochondria requires products from both the nuclear and mitochondrial genomes. The latter contributes a minimal genetic system dedicated to the expression of about a dozen polypeptides, most of which are components of the oxidative phosphorylation apparatus. Alterations in mitochondrial function and mitochondrial damage have been linked to a variety of cellular and organismal responses including apoptosis, neuromuscular disease, tumor pathogenesis, and aging (Green and Reed, 1998; Cortopassi and Wong, 1999; Wallace, 1999; Baysal *et al.*, 2000).

In the budding yeast, *Saccharomyces cerevisiae*, mitochondrial DNA (mtDNA) is dispensable for growth as long as cells are supplied with a fermentable carbon source. This provides a convenient experimental system for analyzing how cells respond to changes in the functional state of mitochondria. One such response is retrograde regulation, a pathway of interorganelle communication whereby the expression of some nuclear genes is altered in cells with dysfunctional mitochondria (Parikh *et al.*, 1987). In cells lacking mtDNA (ρ^o petites), for example, expression of the *CIT2* gene encoding a peroxisomal isoform of citrate synthase is dramatically up-regulated (Liao *et al.*, 1991). *CIT2* expression is dependent on a set of nonessential genes, *RTG1*, *RTG2,* and *RTG3*, which are central players in the retrograde response pathway (Liao and Butow, 1993; Jia *et al.*, 1997). The expression of four other genes, *CIT1*, *ACO1*, *IDH1,* and *IDH2*, encoding TCA cycle enzymes that lead to the synthesis of α-ketoglutarate (α-KG), is also dependent on the *RTG* genes, but only in cells with compromised or dysfunctional mitochondria (Liu and Butow, 1999); in cells with robust mitochondrial function, expression of those genes is dependent on the Hap 2,3,4,5 transcription complex. Glutamate, a precursor to nucleotides and other amino acids, is synthesized directly from the TCA cycle intermediate α-KG and is a potent inhibitor of *RTG*-dependent gene expression (Liu

[V] Online version of this article contains video material and is available at www.molbiolcell.org.

Present addresses: †Aventis Pharmaceuticals, Inc., Cambridge Genomics Center, Cambridge, MA 02139. ‡Molecular Staging, Inc., Guilford, CT 06437.
‖ Corresponding author. E-mail address: butow@swmed.edu.

and Butow, 1999). Thus, glutamate levels may be a key signaling component in the retrograde response pathway.

RTG1 and *RTG3* encode bHLH/Zip transcription factors that activate target gene transcription by binding as a complex to a novel upstream activation sequence called an R box (GTCAC) (Jia *et al.*, 1997). *RTG2* encodes a protein with an N-terminal ATP binding domain similar to the hsp70/actin/sugar kinase superfamily (Bork *et al.*, 1992). Although the biochemical activity of Rtg2p is unknown, it is required for the translocation of Rtg1p and Rtg3p from the cytoplasm to the nucleus when the retrograde response is activated (Sekito *et al.*, 2000). The retrograde response pathway and *RTG2* in particular have been implicated in yeast aging: ρ^o cells with a robust retrograde response have a significantly longer life span than their ρ^+ counterparts, and that life span extension requires *RTG2* (Kirchman *et al.*, 1999). These findings suggest that the retrograde response may affect a broad range of cellular activities.

To obtain a more comprehensive view of cellular responses to mitochondrial dysfunction and to identify potential downstream targets of *RTG1*, *RTG2,* and *RTG3*, we used cDNA-based microarrays to examine genome-wide changes in gene expression induced by a variety of mitochondrial perturbations and by inactivation of *RTG1*, *RTG2,* and *RTG3*. Our results suggest that, to overcome the absence of a complete TCA cycle in respiratory-deficient cells, metabolism has been reconfigured by activation of peroxisomal activities and by reactions that serve to maintain supplies of biosynthetic intermediates (i.e. anaplerotic pathways). The activation of only some of these pathways is dependent on the *RTG* genes. The increase in peroxisomal activity inferred from transcript profiling was confirmed by the direct observation that respiratory deficiency is an inducer of peroxisome biogenesis.

MATERIALS AND METHODS

Yeast Strains and Growth Conditions

Except as noted, strain PSY142 (*MATα leu2 lys2 ura3*ρ^+) and its isogenic derivatives were grown at 30°C in YP (1% yeast extract, 2% bacto peptone, Difco, Detroit, MI) 2% raffinose medium. The ρ^o derivatives were obtained by several passages of ρ^+ cells in YP dextrose medium containing 20 μg/ml ethidium bromide. For plating assays (Figure 3) and microarray experiments evaluating the effect of added propionate, YNB plus cas medium (0.67% yeast nitrogen base supplemented with 1% casamino acids) was used. Acid-treated YNB media were adjusted to pH 5.5 with 5 N KOH before autoclaving. Null alleles of *rtg1*, *rtg2*, and *rtg3* were *LEU2* disruptants described previously (Rothermel *et al.*, 1995; Liu and Butow, 1999). *PDH1* was deleted in strain CEY1131 (**a**/*α his3*Δ*1/his3*Δ*1 ura3*Δ*0/ura3*Δ*0 LEU2/leu2*Δ*0* LYS2/*lys2*Δ*0 TRP1/trp1*Δ*63)* derived from "designer deletion" strains isogenic with the S288C background (Brachmann *et al.*, 1998) by transplacement with *URA3* using *PDH1-URA3* hybrid primers for polymerase chain reaction (PCR) amplification of *URA3*. The deletion was confirmed by Southern blotting of haploid Ura$^+$ segregants. The plating assay (Figure 3, B and C) was performed on a haploid segregant, YCE1131-11-4C (MAT*α pdh1*Δ::*URA3 leu2*Δ*0 his3*Δ*1 ura3*Δ*0 lys2*Δ*0*) and a Ura$^+$ PDH1 control with identical auxotrophies (CEY1118-3B). Strain MMYO11-GFP-AKL (*MATα ura3-1 leu2-3, 112 his3-1 trp1-1 can1-100 ade2::GFP-AKL*) contains two tandem copies of the coding region of green fluorescent protein (GFP) with a C-terminal AKL extension (Marshall *et al.*, 1996) under control of the constitutive *PGK1* promoter integrated into the *ADE2* locus.

RNA Isolation and Northern Blot Analysis

RNA isolation for microarrays and Northern blots was performed as described by Kohrer and Domdey (1991). Northern blots were done essentially as described by Liu and Butow (1999).

Microarray Analysis

Microarrays consisting of 6219 yeast genes were prepared essentially as described by DeRisi *et al.* (1997) and were based on PCR amplification of S288C yeast genomic DNA using gene-specific oligo pairs supplied by Research Genetics (Birmingham, AL). A custom-built spotting robot was used (http://pompous.swmed.edu/exptbio/microarrays/index.htm). PCR was performed with 10 cycles of melting for 15 s at 94°C, annealing for 30 s at 54°C, and extension for 4 min at 68°C, followed by 25 cycles in which extension time was increased by 20 s per cycle. The PCR reaction mixture contained 10 mM Tris-Cl (pH 8.3), 50 mM KCl, 1.5 mM $MgCl_2$, 0.2 μM each oligo, 0.15 ng/μl genomic DNA template, 0.2 mM each deoxyribonucleotide triphosphate, 0.025 U/μl TAQ (Life Technologies, Grand Island, NY), and 0.0001 U/μl Pfu polymerase (Stratagene, La Jolla, CA). For the 192 longest genes in the genome (those exceeding 4073 base pairs [bp] in length) we prepared and arrayed additional PCR products using custom oligos designed to amplify 342–859 bp (average length = 458 bp) near the 3′-end of the open reading frame. Before arraying, we analyzed all of the DNAs by agarose gel electrophoresis, to confirm PCR success and product lengths. Overall, from the 6219 Research Genetics oligo pairs, we found 3% PCR failures and an equivalent rate of trace yields (<13 ng/μl spotted on the array).

Numerical Analyses

The web companion to this article (containing all numerical data and graphical images of raw data) may be found at http://hamon.swmed.edu/butow__array/petite.html. Methods for background subtraction, low value rejection, and normalization are described in detail elsewhere (Epstein *et al.*, 2000) and are available at the above web site.

Each perturbation described in this paper is represented by a pair of replicate hybridizations (two microarrays). For each gene, we computed the signed geometric mean (SGM) response, defined as the antilog of the root mean square of the two log expression ratios; however, we assign a negative value to the geometric mean log ratio before taking the antilog when both log ratios are negative (consistent down-regulation) and assign a value of 1 when the two observations are of opposite sign (discrepant response). To restrict more stringently the genes we consider to be part of a response set, we require a twofold change in SGM response from both early and late logarithmic phase growth (ρ^+ versus ρ^o; Table 1A) or from both 1- and 2-h time points (antimycin and oligomycin; Table 2A). In the case of carbonyl cyanide m-chlorophenylhydrazone (CCCP) treatment (Table 2A), we consider a gene to be part of the response set based on a single SGM of replicate hybridizations, but we use a slightly higher threshold (2.19-fold change) to render the size of the CCCP response set approximately the same as the oligomycin and antimycin response sets.

The Cluster and TreeView programs (Eisen *et al.*, 1998) were used to make Figures 1 and 5, using uncentered correlation as the similarity metric for average linkage clustering. For cluster analysis, we analyzed the unaveraged, normalized expression ratios and included all genes showing at least a threefold change in at least two hybridizations.

To evaluate the probability that the genes jointly affected by two perturbations would arise by chance alone (Table 2B), we computed the expectation of the size of the overlapping set as the product of the fractional representation of the genome in each of the component sets, multiplied by the size of the genome (~6200). The expectation was compared with the actual size of the overlapping set based on χ^2.

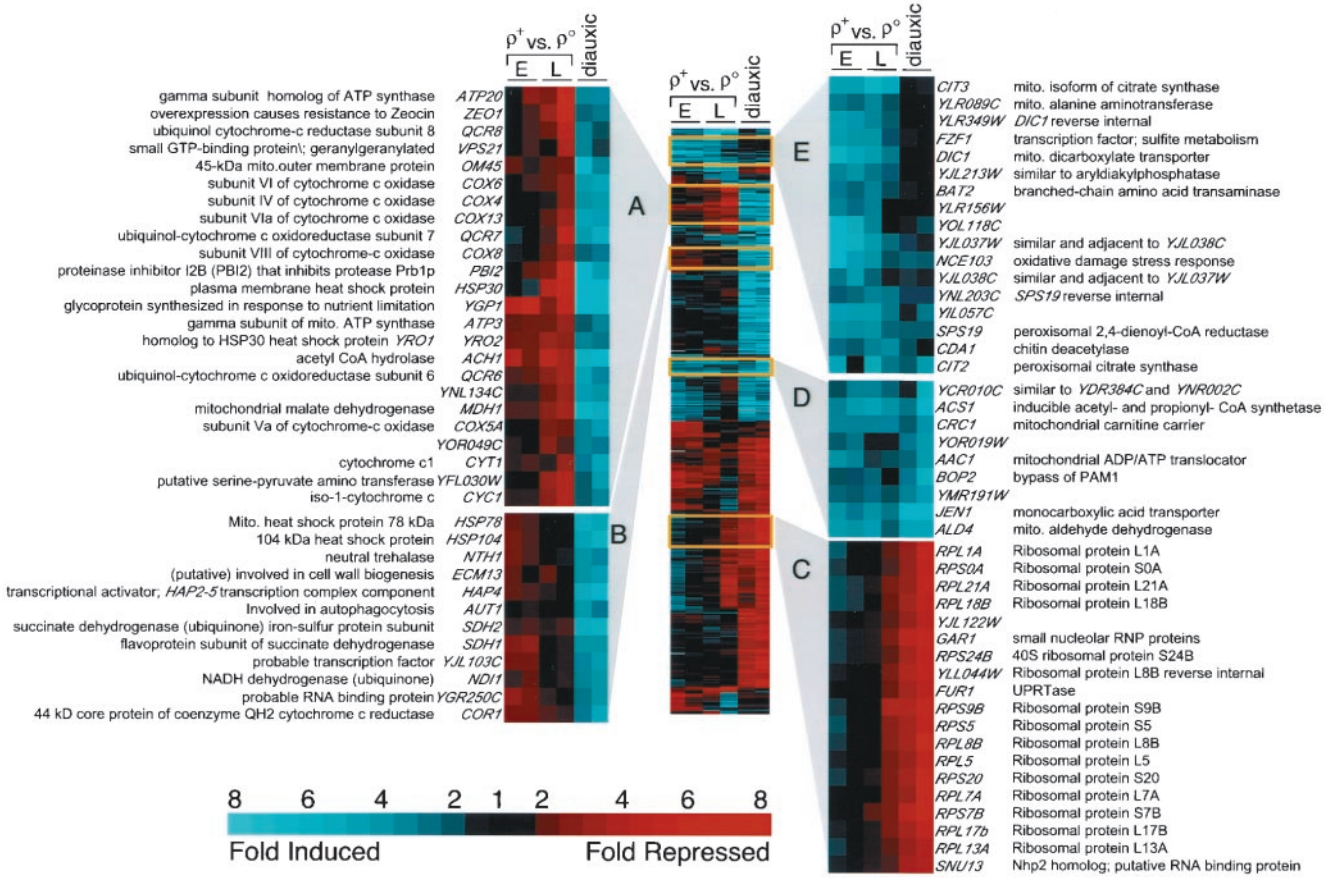

Figure 1. 2-D cluster analysis of gene expression in ρ^o versus ρ^+ cells. The first four columns from left to right are replicate hybridizations of cDNAs prepared from early (E; OD_{600} = 0.5) and late (L; OD_{600} = 1.5) log phase cultures of ρ^+ versus ρ^o cells differentially labeled with Cy3 and Cy5. Data from DeRisi *et al.* (1997) for the last two time points in the diauxic shift of glucose-grown ρ^+ cells (OD_{600} = 6.9 and 7.3) are included in the last two columns on the right, indicated as diauxic. All 402 genes showing at least a threefold change in at least two hybridizations are shown. Blue denotes genes induced in ρ^o relative to ρ^+ or induced during the diauxic shift, and red refers to repressed genes. Mito, mitochondrial; RNP, ribonucleoprotein; UPRT, uracil phosphoribosyl transferase.

Inhibitors of Oxidative Phosphorylation

Antimycin A (Sigma, St. Louis, MO; A-8674), oligomycin (Sigma O-4876), or CCCP (Sigma C-2759) were added to log phase cultures of ρ^+ cells at final concentrations of 1, 3 and 4.1 μg/ml, respectively. Cells from a portion of the culture were harvested for RNA preparation at an OD_{600} of 0.68 (antimycin) or 0.5 (oligomycin and CCCP), and the remaining cells were treated with the inhibitor. Additional samples were collected after ~1 and 2 h of further culture for oligomycin and antimycin or after 1.5 h for CCCP. Labeled cDNAs prepared from each inhibitor-treated culture were mixed with labeled cDNA from the zero-time controls for microarray analysis.

Microscopy

Early log phase cells of strain PGK1-GFP-AKL grown at 30°C in YP 2% raffinose medium were fixed by addition of methanol-free formaldehyde to 4% (vol/vol). After 10 min, the cells were collected by centrifugation at 700 × *g* and resuspended in phosphate-buffered saline (PBS) with 4% formaldehyde for 1 h. Fixed cells were washed four times in PBS and stained for 15 min with 2 μg/ml Calcofluor White (Sigma, Saint Louis, MO) in PBS followed by three washes in PBS. Three microliters of cells were mounted on 2% agarose pads in water (Waddle *et al.*, 1996). Three-dimensional images (28- × 0.108-nm steps) were collected, contrast scaled to 0–255 intensity levels using a range from 0 to 1500, and projected into a single focal plane using the maximum intensity at a given pixel. Overlays between the GFP and Calcofluor images were done using custom software (EditView4D, http://hamon.swmed.edu/~jwaddle/).

For time-lapse microscopy, 3 μl of log phase cells grown at 25°C on YP 2% raffinose medium were mounted on 3% agarose pads containing YP 2% raffinose (Waddle *et al.*, 1996). Where indicated, metabolic inhibitors were added to the culture and to the molten agarose solution (~65°C) just before mounting. Microscopy was performed on an Olympus BMAX-60F with Nomarski differential interference contrast (DIC) and fluorescence optics, a 60× 1.4 NA UPlanApo lens with additional 1.6× magnification, a Princeton Instruments charge-coupled device (EEV-37-BFT), and shutters, filter wheels, and focus control from Ludl Electronic Products (Hawthorne, NY). Automated microscopy was performed with custom software (Jimage4D; complete description of hardware and software can be accessed at http://hamon.swmed.edu/~jwaddle/jimage4d.html). For each experiment, cells in a 35- × 35- × 9-μm^3 volume (135 nm/pixel) were imaged every 15 min for 8–12 h. Neutral density filters blocked

95 and 98.5% of the incident light from the xenon and halogen lamps, respectively. A 250-ms exposure was used for each optical channel. Primary image data were stored as sequentially numbered files, each a stack of images at a given time point, at the full dynamic range of the camera (4096 intensity levels). The images were corrected for uneven illumination and camera bias and then scaled to 8 bits/pixel using a fixed, linear gray scale from 50 to 255. Values >255 were set to white, those <50 to black. Using these image acquisition and scaling parameters, GFP fluorescence from a $\rho+$ strain is barely visible above background, while the ρ^o strain produces bright, fluorescence patches. To produce movies, fluorescence from a given volume was projected into a single 2-D image and then positioned to the right of an equatorial slice from the DIC image stack. The DIC-fluorescence image pairs were then placed into a new stack to view the movie in time-lapse mode, or further montaged with the DIC-fluorescence pair stacks from other movies. QuickTime movies of each can be viewed at http://hamon.swmed.edu/~jwaddle/scratch/.

RESULTS AND DISCUSSIONS

Differential Gene Expression between ρ^+ and ρ^o Petite Cells

To identify genes whose expression changes as a result of mitochondrial dysfunction, we first carried out microarray analysis of the differential, genome-wide expression profile of a respiratory-competent ρ^+ strain versus an isochromosomal ρ^o petite derivative. Two independent pairs of ρ^+ and ρ^o cultures grown in rich medium containing 2% raffinose, a nonrepressing carbon source, were analyzed, with one pair harvested in early (OD_{600} = 0.5) and the other pair harvested in late (OD_{600} = 1.5) logarithmic growth phase. Because we are comparing partially oxidative and obligatorily fermentative strains both grown under derepressing conditions, we elected to compare our results with a transcript profile based on a comparison of robustly oxidative versus fully fermentative, glucose-repressed ρ^+ yeast cultures. Complete data of this sort are available from the experiments of DeRisi *et al.* (1997), who documented the genome-wide changes in gene expression of yeast cells undergoing the transition from glucose fermentative to oxidative metabolism—the diauxic shift. Many proteins, including enzymes of oxidative metabolism, become derepressed during the diauxic shift, reaching a maximum level of expression when the glucose is exhausted from the medium and the cells are utilizing ethanol for growth.

To present our results, we used a 2-D clustering algorithm (Eisen *et al.*, 1998) that groups similarly responsive genes and displays them as a two-color graphic with color intensities proportional to the fold change in gene expression (Figure 1). Selected regions of the cluster representation have been magnified to display groups of genes in the ρ^+-ρ^o comparison and the late diauxic shift. Figure 1, clusters A and B, represent a group of genes that are down-regulated in ρ^o cells and up-regulated in cells that have switched from fermentative to oxidative metabolism. A large proportion of the genes in this group encode mitochondrial proteins of the oxidative phosphorylation apparatus, such as subunits of the cytochrome *c* oxidase and ATP synthase complexes. These data imply that petites make no (futile) attempt to compensate for their respiratory-deficient state by up-regulating the expression of oxidative phosphorylation genes. This contrasts with the observation that some genes of the oxidative phosphorylation apparatus are up-regulated in human cells harboring deleterious mtDNA mutations (Heddi *et al.*, 1999). In those cases, mitochondrial gene expression was also elevated, suggesting activation of a general pathway of increased mitochondrial biogenesis to compensate for mitochondrial dysfunction.

Figure 1, cluster C, contains mainly cytoplasmic ribosomal protein genes, which are substantially down-regulated in the diauxic shift (DeRisi *et al.*, 1997), and which show an interesting difference in their regulation between early and late logarithmic phase ρ^o cultures. Coordinate down-regulation of genes involved in ribosome biogenesis is generally observed in cells as growth rate slows, as in the diauxic shift, e.g., when there is a switch from an optimal carbon source (glucose) to a poor one (ethanol) (DeRisi *et al.*, 1997). In medium containing 2% raffinose, the doubling time of ρ^o petite cells is ~40–50% of their isochromosomal ρ^+ counterparts. Nevertheless, these same ribosomal protein genes are apparently down-regulated in ρ^o cells only when those cells traverse late logarithmic phase.

Figure 1, clusters D and E, represent a group of genes whose expression is up-regulated in ρ^o petites and, for the most part, in cells late in the diauxic shift. Most of the genes within this group, which includes *CIT2*, are involved in intermediary metabolism and small molecule transport pathways. This group is potentially the most interesting class of genes whose expression is affected in ρ^o petite cells, because differences in their expression could reflect metabolic changes that would compensate for the loss of respiration.

As a further refinement of the analysis of genes up-regulated in ρ^o petites, we focus on those genes whose geometric mean expression level (defined in MATERIALS AND METHODS) increased at least twofold in both the low and high OD replicate comparisons of ρ^+ and ρ^o cultures; these are the genes whose expression is consistently affected by the ρ^o mitochondrial genotype in a cell density-independent manner. By these criteria, we identified 43 genes that are up-regulated in the respiratory-incompetent ρ^o petite cells (Table 1A).

Transcript Profiling Suggests Metabolic Remodeling in Respiratory-deficient Cells

Intermediates of the TCA cycle are required for the biosynthesis of amino acids and nucleotides. Because part of the TCA cycle (succinate oxidation) cannot proceed in respiratory-deficient cells, oxaloacetate (OAA) is not regenerated and must therefore be supplied stoichiometrically. The genome-wide transcript profile suggests that metabolism in ρ^o cells has been reconfigured to provide increased supplies of OAA and its condensation partner, acetyl-CoA for these biosynthetic reactions (Figure 2 and Table 1A). For example, the expression of *PYC1,* encoding pyruvate carboxylase, which catalyzes the synthesis of OAA from pyruvate and CO_2, and *ACS1,* encoding an acetyl-CoA synthase, are up-regulated in ρ^o petites. *ACH1*, however, which encodes an acetyl-CoA hydrolase, is strongly down-regulated in these cells. Additionally, many of the genes up-regulated in ρ^o cells encode proteins that function in the conversion and flux of metabolites generated from β-oxidation of fatty acids (a peroxisomal activity in yeast) to intermediates of the TCA and glyoxylate cycles (Figure 2). The central role of the

Table 1A. Genes induced in respiratory-deficient cells

Open reading frame	Gene	Fold change in ρ^o	Fold change in antimycin	Oleate induction	Function
YJL037W		7.1	5.2		Similar and adjacent to YJL038C
YDR384C		5.9	4.6	see YCR010C	Similar to YNR002C and YCR010C
YPR002W	*PDH1*	5.8	9.43		Propionate catabolism
YPR001W	*CIT3*	5.2	12.7		Mitochondrial isoform of citrate synthase
YCR005C	*CIT2*	5.1	10.0	+	Peroxisomal citrate synthase
YFL011W	*HXT10*	5.0	4.5		High-affinity hexose transporter
YLR348C	*DIC1*	5.0	5.3		Mitochondrial dicarboxylate transporter
YAL054C	*ACS1*	4.2	6.2	+	Inducible acetyl- and propionyl-CoA synthetase
YIL057C		4.2	24.6	+	
YPL265W	*DIP5*	4.2	3.2		Dicarboxylic amino acid permease
YNL036W	*NCE103*	4.0			Oxidative damage stress response
YLR307W	*CDA1*	4.0			Chitin deacetylase
YOR374W	*ALD4*	3.7		+	Aldehyde dehydrogenase
YBR296C	*PHO89*	3.6			Na^+ phosphate symporter
YOR100C	*CRC1*	3.5	5.8		Mitochondrial carnitine carrier
YLR349W		3.5			DIC1 reverse internal
YKL217W	*JEN1*	3.5	2.8	+	Monocarboxylic acid transporter
YNL202W	*SPS19*	3.4	3.2	+	Peroxisomal 2,4-dienoyl-CoA reductase
YGL254W	*FZF1*	3.4			Transcription factor; sulfite metabolism
YJL213W		3.3			Similar to arylidialkylphosphatase
YMR303C	*ADH2*	3.1			Alcohol dehydrogenase II
YCR010C		3.0	12.2	+	Similar to YDR384C and YNR002C
YNR060W	*FRE4*	3.0			Similar to ferric reductase; electron transport
YGR260W	*TNA1*	3.0			Nicotinic acid transporter
YGL062W	*PYC1*	2.9			Pyruvate carboxylase
YNL203C		2.8	3.2		
YLR089C		2.6			Mitochondrial alanine aminotransferase
YPL147W	*PXA1*	2.6	6.3	+	ABC family long-chain fatty acid transporter
YBR105C	*VID24*	2.5			Peripheral vesicle membrane protein
YJR148W	*BAT2*	2.5			Branched-chain amino acid transaminase
YOL147C	*PEX11*	2.4	2.8	+	Peroxisome biogenesis
YER187W		2.3			
YLR004C		2.3			Similar to allantoate permease
YNL012W	*SPO1*	2.3			Similar to phospholipase B
YPL281C	*ERR2*	2.2			Similar to enolase
YDL174C	*DLD1*	2.2			Mitochondrial D-lactate dehydrogenase
YOL119C		2.2			Potential monocarboxylate transporter
YPL018W	*CTF19*	2.2	3.2		Kinetochore protein
YAR068W		2.2			
YMR191W		2.2	3.1		
YNL279W		2.2			
YOL059W	*GPD2*	2.1			Glycerol-3-phosphate dehydrogenase (NAD+)
YBR132C	*AGP2*	2.1			Carnitine transport across plasma membrane

peroxisomes in these metabolic interconversions is also reflected by the finding that 13 of the up-regulated genes indicated in Table 1A are localized to the peroxisome, induced by oleate (a potent peroxisomal proliferator), or support peroxisomal activities (Veenhuis *et al.*, 1987; Kunau *et al.*, 1988; Skoneczny *et al.*, 1988).

Crucial to the replenishment of acetyl-CoA and OAA, and metabolites derived from OAA, is their transport from extramitochondrial sources to mitochondria. This transport requires carboxylic acid carriers and acylcarnitine transferases. It is striking therefore that in ρ^o cells there is an up-regulation of expression not only of *DIC1*, encoding a mitochondrial dicarboxylic acid transporter, and *CRC1*, encoding an inner mitochondrial membrane acylcarnitine transporter, but of *AGP2*, which encodes a plasma membrane carnitine transporter. It has been suggested that yeast cells are unable to synthesize carnitine de novo and must therefore rely on extracellular sources of carnitine to provide the substrates for the acylcarnitine carriers (van Roermund *et al.*, 1999). The up-regulation of *CIT2* could provide additional citrate directly from the glyoxylate cycle and the OAA replenished by OAA derived from the pyruvate carboxylase reaction.

Because petite cells lack mitochondrial electron transport and are therefore dependent on glycolysis for biomass and energy, they require alternative mechanisms for reoxidation of NADH. The major pathways for these steps in nonoxidative cells would be α-glycerol-3-phosphate and alcohol dehydrogenase activities. Genes encoding enzymes carrying out these reactions, *GPD2* and *ADH*, are both up-regulated

Table 1B. Oleate-inducible genes up-regulated uniquely after both 1 and 2 h of antimycin treatment

Open reading frame	Gene	Fold change in antimycin	Function
YFL014W	*HSP12*	13.2	12-kDa heat shock protein
YKR097W	*PCK1*	8.7	Phosphoenolpyruvate carboxykinase
YGL205W	*POX1*	7.8	Fatty acyl-CoA oxidase
YDR256C	*CTA1*	5.2	Peroxisomal catalase A
YKR009C	*FOX2*	4.0	Peroxisomal beta-oxidation protein
YOL052CA	*DDR2*	3.1	Induced by DNA damage and diverse stress
YNL009W	*IDP3*	2.8	Peroxisomal NADP-dependent IDH

Genes induced in ρ^o petite and antimycin treated cells. (A) All genes induced in ρ^o petites by at least 2-fold in both early and late logarithmic phase cultures. The average of the early and late log phase transcriptional responses is shown. Respiratory competent ρ^+ cells were treated with 1 μg/ml of antimycin. The average response to antimycin treatment is also shown for the subset of genes that were affected by antimycin treatment after both 1 and 2 h of treatment. Functional descriptions were adapted from YPD Proteome and SGD data bases (Costanzo *et al.*, 2000; Cherry *et al.*, 1998). (B) All oleate induced genes (Kal *et al.*, 1999) induced uniquely after both 1 and 2 h of antimycin treatment. The averages of responses after 1 and 2 h of treatment are shown.

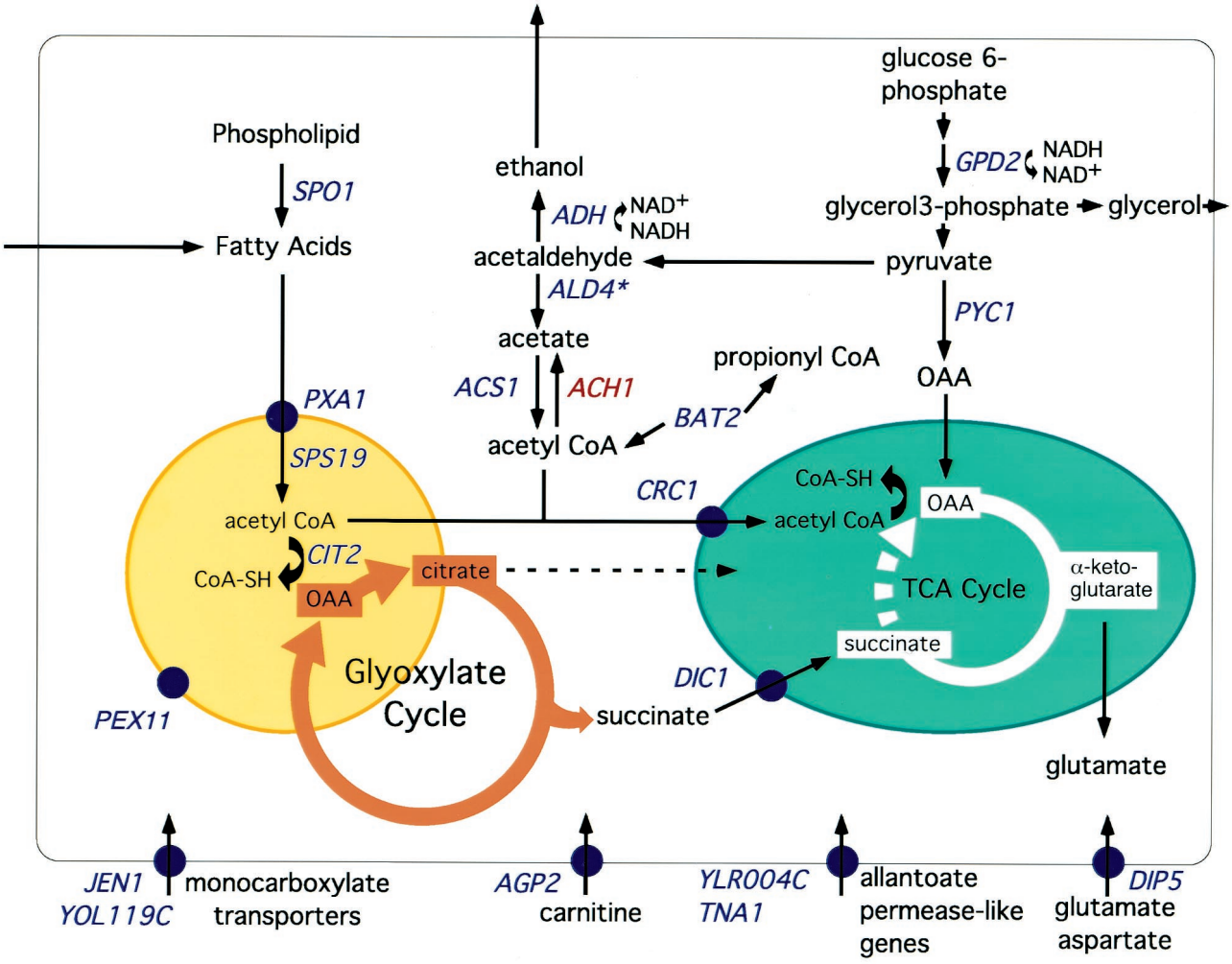

Figure 2. Metabolic pathways affected in respiratory-deficient cells as inferred from transcript profiling. Nineteen of the 34 genes induced in ρ^o petites (Table 1A) and having some functional description are indicated in blue. Also included in the display in red is *ACH1*, whose expression is strongly down-regulated in ρ^o cells. A peroxisome is indicated by the yellow circle and a mitochondrion by the green ellipse. TCA cycle flux from succinate to OAA is blocked (broken line) in respiratory-deficient cells. Gene products associated with a particular membrane are indicated by blue circles. On our array, the spots for *ADH1* and *ADH2* both showed induction in ρ^o cells. However, because of 157 nucleotides of contiguous identity between these two genes, transcripts of *ADH1* and *ADH2* cannot be distinguished by microarray probes targeting entire reading frames.

in those cells. In addition, the array data suggest that the ρ^o petite cells have further optimized nutrient availability by up-regulation of transporters for amino acids (*DIP5*), poor nitrogen sources (*TNA1* and *YLR004C*), sugars (*HXT10*), and monocarboxylic acids (*JEN1* and *YOL119C*). Finally, ρ^o petites up-regulated two amino acid transaminases, *BAT2* (branched chain amino acids, see below) and *YLR089C* (a potential mitochondrial alanine amino transferase) that would lead to increased supplies of pyruvate, acetyl-CoA, and propionyl-CoA. In summary, transcript profiling suggests that, to overcome blocks in the TCA cyle, ρ^o petites reconfigure metabolism by recruiting peroxisomal activities, small molecule transport systems and lipid, sugar, and amino acid turnover to increase the availability of OAA, acetyl-CoA, and propionyl-CoA for biosynthetic reactions.

Genes That May Function in Propionate Metabolism

One of the genes whose expression in respiratory-deficient cells most closely correlates with *CIT2* is *PDH1* (*YPR002W*). Coregulation of expression of these genes in cells with certain mitochondrial perturbations has also been noted recently by Hughes *et al.* (2000). *PDH1* is 62% identical to the prpD genes of *Escherichia coli* and *Salmonella typhimurium,* which play an unknown but essential role in propionate catabolism (Horswill and Escalante-Semerena, 1997; Textor *et al.*, 1997). Given that ρ^o cells also up-regulate *BAT2*, which leads to the production of propionyl-CoA as a product of valine and isoleucine catabolism (Figure 2) and *ACS1*, the acetyl-CoA synthase isoform that also functions as a propionyl-CoA synthase (van den Berg *et al.*, 1996), we investigated a possible role for *PDH1* in propionate metabolism. We confirmed by Northern blot analysis that *PDH1* is strongly induced in early, middle, and late log phase cultures of ρ^o petites, in a manner similar to *CIT2* (Figure 3A).

Exogenous propionate reportedly augments the growth of yeast in glucose-limited, aerobic chemostat cultures (Pronk *et al.*, 1994) but is toxic under anaerobic conditions (Verduyn *et al.*, 1990), presumably because the energetic stress of anaerobiosis exceeds the capacity of the plasma membrane ATP-dependent proton pump to excrete H^+ efficiently when propionic acid is taken up by cells. We deleted *PDH1* and determined the effects of propionate on the growth of the wild type and *pdh1*Δ strains cultured in medium containing low concentrations of raffinose to limit the energy supply. Below 0.2% raffinose, 50 mM propionate is far more toxic to *pdh1*Δ than to wild-type cells (Figure 3B). In contrast, 50 mM acetate augments the growth of both wild type and *pdh1*Δ strains grown in limiting raffinose (Figure 3C), demonstrating that *pdh1*Δ cells are specifically sensitive to propionate treatment. These data suggest that *PDH1* functions in propionate utilization in yeast.

Yeast and *E. coli* appear to catabolize propionate via the methyl citrate pathway, which results in a net partial oxidation of propionate to pyruvate (Pronk *et al.*, 1994); (Textor *et al.*, 1997). The methyl citrate pathway proceeds by reactions resembling the synthase, isomerase, and lyase steps of the glyoxylate cycle, followed by the regeneration of OAA from succinate via the TCA cycle (Tabuchii *et al.*, 1974). However, the genes encoding the enzymes that metabolize propionate in *S. cerevisiae* have not been determined. We used microarrays to compare transcripts between wild-type yeast grown

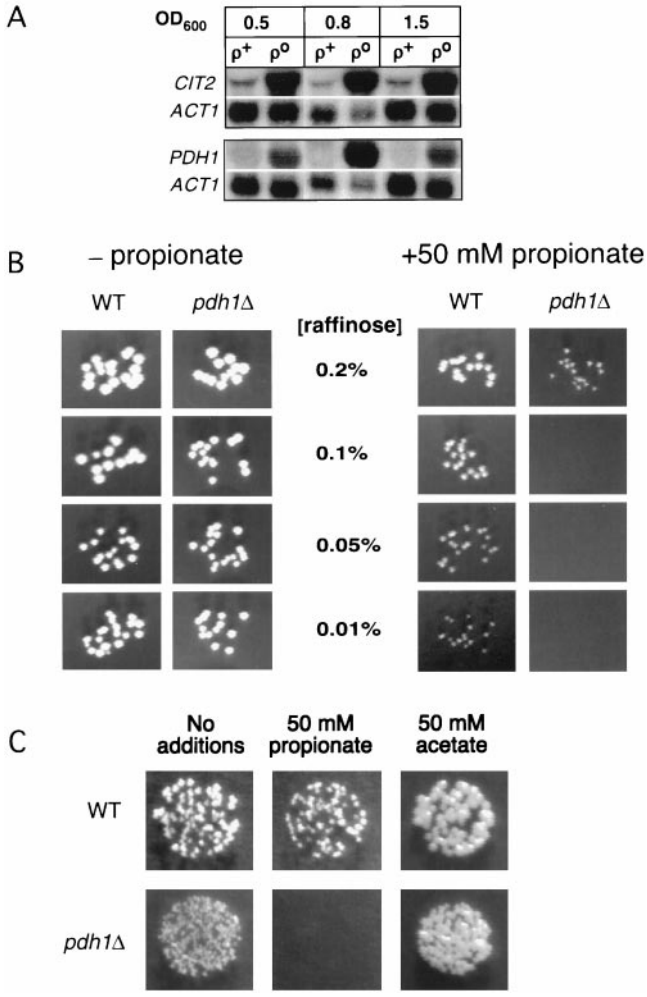

Figure 3. *PDH1* is a retrograde regulated gene and may function in propionate metabolism. (A) Northern blots showing increased abundance of *PDH1* and *CIT2* transcripts in ρ^o compared with ρ^+ cells at three different cell densities. (B) Growth of wild-type (WT) and *pdh1*Δ cells on YNB 1% casein medium with or without propionate and containing limiting amounts of raffinose as indicated. (C) Growth of wild-type (WT) and *pdh1*Δ cells on YNB, 1% casein, 0.05% raffinose medium with or without propionate or acetate as indicated.

in 2% raffinose medium with or without supplemental 50 mM propionate. We found a strong induction of *PDH1*, *CIT3* (but not *CIT2* or *CIT1*), *ACO1* (but not *YJL200C*), and *ICL2* (but not *ICL1*) in response to propionate (data available at http://hamon.swmed.edu/butow__array/petite.html). The organic acid-transporting ATPase, *PDR12*, was also dramatically induced, consistent with the model for propionate toxicity under conditions of energy limitation mentioned earlier (Verduyn *et al.*, 1990). Possibly, *CIT3*, *ACO1*, and *ICL2* perform the anticipated synthase, isomerase, and lyase steps of the methyl-citrate pathway, and *PDH1* plays an as yet undefined role in propionate metabolism. Interestingly, *PDH1* orthologs in prokaryotic operons are adjacent to a citrate synthase-like gene (prpC) whose production was shown to have methyl citrate synthase activity (Textor *et al.*,

1997), and in yeast, *PDH1* is adjacent to *CIT3* on chromosome VI. The induction of *ACS1*, *BAT2*, *CIT3*, and *PDH1* in ρ^o petites may represent a further example of the metabolic reorganization of respiratory-deficient cells, with branched chain amino acid turnover leading to propionyl-CoA and ultimately to pyruvate via the methyl citrate pathway.

Different Mitochondrial Inhibitors Elicit Different Genome-wide Responses in Gene Expression

The absence of oxidative phosphorylation in ρ^o cells is the result of their failure to synthesize components of both the mitochondrial electron transport chain and the ATP synthase complex. To gain insight into the effects of specific, acute perturbations of mitochondrial function on global patterns of gene expression, we exposed ρ^+ cells to three different inhibitors of oxidative phosphorylation—antimycin, CCCP, and oligomycin. The effects of these inhibitors on mitochondrial function are well documented, and they are known to inhibit oxidative phosphorylation in fundamentally different ways. Antimycin is a specific inhibitor of mitochondrial electron transport, blocking the reoxidation of reduced cytochrome *b*. CCCP uncouples electron transport from ATP synthesis by enabling free movement of protons across the inner mitochondrial membrane, resulting in a collapse of the H^+ gradient necessary to drive ATP synthesis via the ATP synthase complex. In contrast to antimycin treatment, cells treated with CCCP have maximal (uncoupled) rates of mitochondrial electron transport activity. Finally, oligomycin is a specific inhibitor of the F0 component of the F1-F0 ATP synthase complex and inhibits both ATP synthesis and ATP synthesis-associated (state 4) respiration.

Log phase cultures of ρ^+ cells grown in YP 2% raffinose medium were treated with antimycin (1 μg/ml), oligomycin (3 μg/ml), or CCCP (4.1 μg/ml). In preliminary experiments we verified that these concentrations were sufficient to inhibit the growth of ρ^+ cells growing nonfermentatively. For microarray analysis, aliquots of cells were removed 1–2 h after the addition of the inhibitors and compared with untreated (zero time point) controls.

Analysis of genes jointly affected by different mitochondrial perturbations shows a striking degree of overlap between the effects of antimycin treatment and ρ^o cells (Table 2): 44% (19 genes) of the 43 genes up-regulated in ρ^o cells are also up-regulated by treatment of ρ^+ cells with antimycin. The 19 genes include 10 of the 13 genes mentioned earlier (Table 1A) having a role in peroxisomal function. Moreover, using stringent criteria for designation of an induced gene (detailed in MATERIALS AND METHODS), we found that several additional genes induced by antimycin are also plausibly part of a pathway of up-regulated peroxisomal function. This set includes *CTA1* (peroxisomal catalase), *FOX2* (peroxisomal β-oxidation protein), *POX1* (fatty acyl-CoA oxidase), and *IDP3* (peroxisomal NADP-dependent isocitrate dehydrogenase; Table 1B). Altogether, a total of 19% (20 genes) of the 106 genes that are up-regulated in ρ^o petites or antimycin-treated ρ^+ cells either are oleate inducible or have some involvement in peroxisomal metabolism.

In contrast with the similarities in gene induction between ρ^o and antimycin-treated cells, very few of the up-regulated genes resulting from CCCP or oligomycin treatment were also up-regulated in ρ^o cells (Table 2A), suggesting that the ρ^o transcript profile is dominated by the effects of loss of electron transport rather than the loss of mitochondrial ATP synthesis per se. Significant overlap was seen between the genes induced in CCCP and both antimycin and oligomycin (Table 2), but there was no obvious pattern that would suggest a coherent biological role for these genes. Although comparable numbers of genes were up-regulated by each of the inhibitors, a much larger number of genes were down-regulated by oligomycin treatment than by treatment with antimycin or CCCP (Table 2A). Little or no significant overlap was found when considering the genes down-regulated in common by these diverse perturbations (Table 2B).

Table 2. Genes showing consistent response to each perturbation

A.

Numbers of upregulated genes

	ρ^o	Antimycin	Oligomycin	CCCP	
	43	19	1	2	ρ^0
		82	3	13	Antimycin
			69	10	Oligomycin
				75	CCCP
ρ^0	20				
Antimycin	0	18			
Oligomycin	3	2	166		
CCCP	0	2	0	67	

Numbers of down-regulated genes

B. Negative log of probability that responses to two perturbations are independent

	ρ^o	Antimycin	Oligomycin	CCCP
ρ^0		131	0	1
Antimycin	0		2	33
Oligomycin	3	2		23
CCCP	0	4	1	

Overlapping effects of four perturbations of mitochondrial respiration and ATP synthesis. (A) Numbers of genes induced or repressed by four perturbations of mitochondrial ATP synthesis and by all pairwise combinations of perturbations. The numbers on the upper and lower main diagonals count the genes induced or repressed, respectively, in each perturbation. The numbers off the main diagonals count the genes induced or repressed by each pair of perturbations. Resipiratory competent ρ^+ cells were treated with either 1 μm/ml antimycin, 3 μg/ml oligomycin, or 4.1 μg/ml CCCP. (B) χ^2 analysis of the overlap between the sets of genes induced or repressed by each of the individual perturbations.

Peroxisome Proliferation in Respiratory-deficient Cells

In ρ^o petites, an intact retrograde pathway is required for oleate induction of peroxisome biogenesis, suggesting a link between mitochondrial dysfunction and peroxisomal activities (Chelstowska and Butow, 1995; Kos *et al.*, 1995). That notion is strengthened by the current experiments, which suggest that peroxisomal activities may play a crucial role in the metabolic remodeling of respiratory-deficient cells. Given that many of the genes up-regulated in ρ^o petites are known to be induced by oleate, we asked whether enhanced peroxisome proliferation also occurs in those cells. For this purpose, we used a strain expressing a chromosomally integrated fusion gene encoding a derivative of GFP with a peroxisomal matrix-targeting signal,

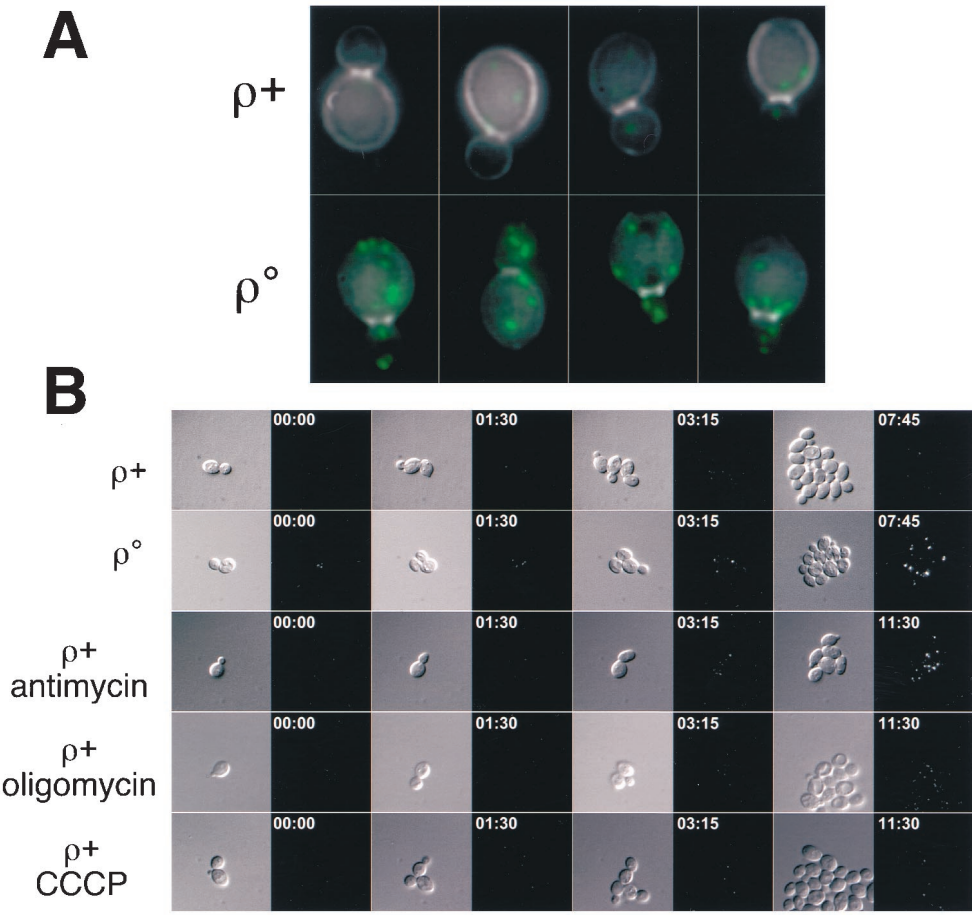

Figure 4. Peroxisome induction in respiratory-deficient cells. (A) Overlay between Calcofluor White staining (gray) and GFP peroxisomal marker (green) in representative ρ^+ and ρ° cells. Each image is a 2-D projection of a 3-D image of the entire cell volume. The images were generated with a fixed exposure time and illumination intensity and a camera with a dynamic range exceeding 3 orders of magnitude. (B) Selected time points from 3-D, time-lapse recordings comparing peroxisome biogenesis in respiratory-competent, respiratory-deficient, and drug-treated cells. The DIC images are taken from an equatorial focal plane, whereas the GFP images are 2-D projections showing all peroxisomes in the image volume above a fixed intensity range. Annotation indicates elapsed time in hours:minutes format from start of experiment. Because the drug-treated cells grow slower than untreated ρ^+ and ρ^o cells, a later time point is used for the final images in the drug-treated samples.

AKL, at its C terminus. This GFP derivative, whose expression is under the control of the constitutive *PGK1* promoter, has been shown to target efficiently and exclusively to peroxisomes and is an accurate indicator of peroxisome proliferation induced by exogenous oleic acid (Marshall *et al.*, 1996). The PGK1-GFP-AKL ρ^+ strain was converted to a ρ^o petite by treatment with ethidium bromide.

Microscopic examination of log phase cultures of the PGK1-GFP-AKL ρ^+ and ρ° strains revealed a dramatic increase in the intensity of peroxisomal profiles, indicative of an increase in peroxisome biogenesis in the ρ° derivative (Figure 4A). When viewed using an intensity range typical for the GFP-AKL fluorescence in ρ° cells, the peroxisomes in ρ^+ cells are nearly undetectable (Figure 4A, top row). It should be noted that peroxisomes in ρ^+ cells are easily visualized when viewed with a more sensitive intensity scaling function. GFP-AKL foci were completely absent in ρ^+ and ρ° derivatives deleted for *pex5* (Epstein, Waddle, Hale, Davé, Thornton, Macatee, Garner, and Butow, unpublished results), a peroxin essential for the import of proteins into the peroxisomal matrix (Vanderleij *et al.*, 1993).

Because transcript profiling suggested that only antimycin treatment of ρ^+ cells had significant similarities to ρ° cells in terms of the up-regulation of oleate inducible genes (Table 2), we tested whether peroxisome proliferation might also be unique to antimycin treatment. Accordingly, we examined peroxisomal profiles using 3-D time-lapse fluorescence microscopy in living, PGK1-GFP-AKL ρ^+ cells treated over a 12-h period with antimycin, oligomycin, or CCCP. The image acquisition parameters were adjusted such that at a constant exposure, excitation level, and intensity scaling ρ^+ peroxisomes in untreated cells are barely detectable, whereas those in ρ° cells are bright, distinct foci (compare first to second row in Figure 4B). In agreement with the results of the transcript profiling, we found a striking antimycin-dependent increase in peroxisomal fluorescence ~3 h after treatment (third image pair, row 3, Figure 4B). The intensity of the peroxisomes in the antimycin-treated ρ^+ cells was nearly indistinguishable from that of ρ^o cells. Moreover, the response was largely specific to antimycin because oligomycin treatment caused only a minor increase in peroxisomal intensity and CCCP-treated cells did not differ from untreated ρ^+ cells. Thus, the involvement of enhanced peroxisomal activities in respiratory-deficient cells inferred from transcript profiling (Figures 1 and 2 and Table 1) was borne out by the observation of enhanced peroxisome biogenesis in those cells (Figure 4). The partial inhibition of electron transport activity by oligomycin may account for the slight increase in peroxisome profiles observed in Figure 4, although no induction of peroxisome-related genes was evident in the transcript profiling that was consistently above the stringent cut-off criteria we have applied in these experiments.

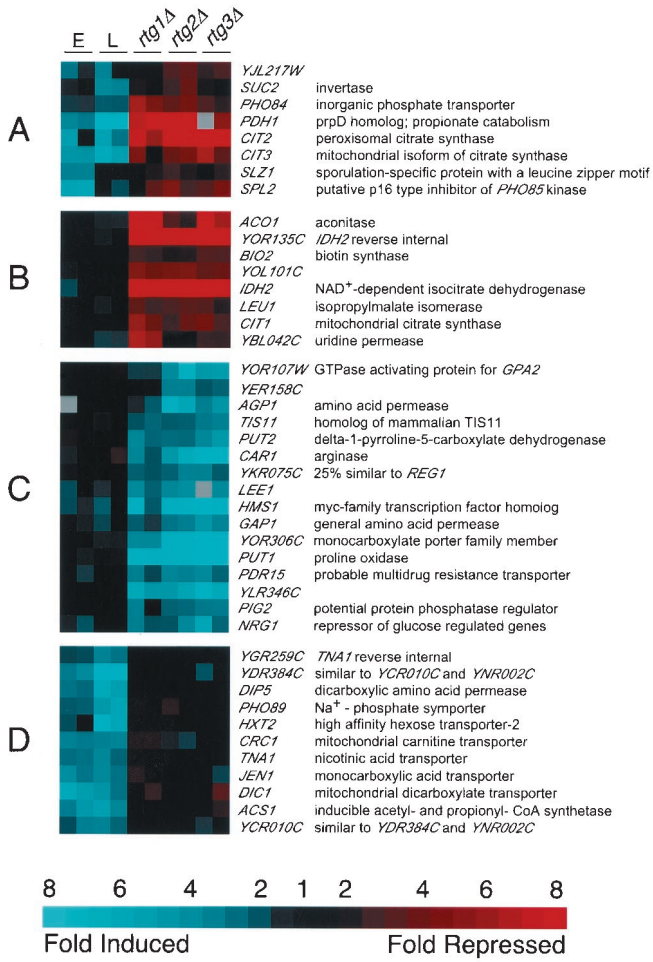

Figure 5. Effects of *RTG* mutations in ρ^o cells. The four columns on the left are replicate comparisons of early (E) and late (L) log phase ρ^+ and ρ^o cultures, as detailed in the legend to Figure 1. The six columns on the right are replicate comparisons of ρ^o cells and ρ^o cells containing deletions of *rtg1*, *2*, or *3*, respectively, and are based on cultures harvested at an OD_{600} = 0.8. (A–C) Genes whose expression is affected by *RTG1*, *2*, and *3* in ρ^o cells. (D) A group of genes induced by respiratory deficiency in an *RTG*-independent manner. Blue refers to genes induced in ρ^o relative to ρ^+ or induced in ρ^o *rtg* relative to ρ^o *RTG*. Red refers to repressed genes. All 273 genes that changed by at least threefold in at least two experiments are shown.

RTG *Genes*

Because of the importance of the *RTG* genes in the retrograde response, we next characterized globally the sets of genes whose expression is influenced by one or more of the *RTG* genes in ρ^o cells. To this end, we obtained transcript profiles from comparisons of an *RTG* wild-type ρ^o strain and *rtg1*Δ, *rtg2*Δ, or *rtg3*Δ ρ^o derivatives and used cluster analysis to elucidate the sets of genes that are sensitive to the *rtg* mutations in the ρ^o background (Figure 5). Figure 5, cluster A, identifies a set of genes that are induced in ρ^o petites and whose induction depends on signaling via the *RTG* pathway. The size of this set is limited and, in addition to *CIT2*, includes *CIT3* and *PDH1* (discussed above). Figure 5, cluster B, presents additional genes that depend on *RTG* genes for their expression in ρ^o cells. Unlike the *CIT2* class (Figure 5, cluster A), these genes are not induced in ρ^o relative to their expression in ρ^+ cells. This set includes *CIT1*, *IDH2*, and *ACO1*, which encode enzymes catalyzing the first three steps of the TCA cycle, leading to α-KG and glutamate, a retrograde regulator. These data are in agreement with a previous study showing that expression of these TCA cycle genes becomes dependent on the *RTG* genes as mitochondrial respiratory function is reduced (Liu and Butow, 1999).

The genes showing enhanced expression in *rtg*Δ ρ^o compared with *RTG* ρ^o cells are illustrated in Figure 5, cluster C. These genes behave as if they were repressed by *RTG* gene activity, but this is probably an indirect response to the exacerbated defects suffered by ρ^o cells when they are also deficient in retrograde signaling. This set of genes includes *PUT1* (proline oxidase), *CAR1* (arginase), *AGP1*, and *GAP1* (both amino acid carriers), which are all involved in amino acid turnover or transport. The strong, consistent induction of *PUT1* and *CAR1* suggests that cells are attempting to up-regulate the synthesis of glutamate from nutritionally derived proline and arginine under circumstances in which combined genetic deficiencies preclude synthesis via α-KG derived from the TCA cycle. Although petites are unable to oxidize proline via proline oxidase encoded by *PUT1*, the synthesis of *PUT1* mRNA is nevertheless subject to regulation in petites (Wang and Brandriss, 1987). Finally, Figure 5, cluster D, illustrates genes that are induced in ρ^o relative to ρ^+ but whose expression in ρ^o cells is nearly independent of the *RTG* genes. Included in this class are membrane carriers for monocarboxylic (*JEN1*) and dicarboxylic (*DIP5*) acids, phosphate (*PHO89*), and hexose (*HXT2*). The induction of these genes suggests that the transcriptional response to mitochondrial dysfunction depends on novel retrograde signaling pathways, in addition to those involving *RTG1*, *RTG2*, and *RTG3*.

CONCLUSION

Transcript profiling suggests that respiratory-deficient yeast cells respond to the loss of oxidative phosphorylation by reconfiguring metabolism to increase supplies of acetyl-CoA and OAA from peroxisomal activities and anaplerotic reactions. Because the TCA cycle no longer functions as a cycle in respiratory-deficient cells, stoichiometric amounts of OAA must be available for condensation with acetyl-CoA. This is to ensure that the first three steps of the TCA cycle, which are under control of the *RTG* genes in cells with compromised mitochondrial function, operate at a rate sufficient to meet cellular demands for glutamate, also a regulator of the retrograde response. Microarray analysis revealed *RTG*-dependent, retrograde-responsive genes that are likely to function in propionate metabolism. Other retrograde-responsive genes, however, were identified that do not appear to be under control of the *RTG* genes, suggesting that new pathways will unfold in mitochondria-to-nucleus signaling. Respiratory-competent ρ^+ cells treated with different inhibitors of oxidative phosphorylation show the induction of overlapping but nonidentical sets of genes. Of the inhibitors, only antimycin treatment induces many of the

same genes induced in ρ^o petites, a number of which are involved in peroxisomal activities. These array data led to a prediction that respiratory deficiency, but not the loss of mitochondrial ATP synthesis per se, would result in an increase in peroxisome biogenesis. Microscopic examination of cells expressing a derivative of GFP with a peroxisomal matrix-targeting signal confirmed these predictions. Future studies should reveal the similarities or differences in the pathway of peroxisome biogenesis induced by respiratory deficiency and by oleate induction.

ACKNOWLEDGMENTS

We thank T. Fonden for oligo design, K. Kupfer for helpful discussions of numerical methods, D. Middelman for software support, and J. Goodman for GFP-AKL strains. We also thank M. Eisen and G. Sherlock for clustering software and V. Iyer and J. DeRisi for advice on microarrays. Finally, we are grateful to M. McCammon for many helpful discussions. This work was supported by National Institutes of Health grants GM22525 and CA77811 and a Robert A. Welch Grant (I-0642) to R.A.B. C.B.E. was supported in part by a Postdoctoral Fellowship (AG05781) from the National Institutes of Health.

REFERENCES

Baysal, B.E., Ferrell, R.E., Willett-Brozick, J.E., Lawrence, E.C., Myssiorek, D., Bosch, A., van der Mey, A., Taschner, P.E., Rubinstein, W.S., Myers, E.N., Richard, C. W., 3rd, Cornelisse, C.J., Devilee, P., and Devlin, B. (2000). Mutations in SDHD, a mitochondrial complex II gene, in hereditary paraganglioma. Science *287*, 848–851.

Bork, P., Sander, C., and Valencia, A. (1992). An ATPase. domain common to prokaryotic cell cycle proteins, sugar kinases, actin and hsp70 heat shock proteins. Proc. Natl. Acad. Sci. USA *89*, 7290–7294.

Brachmann, C.B., Davies, A., Cost, G.J., Caputo, E., Li, J.C., Hieter, P., and Boeke, J.D. (1998). Designer deletion strains derived from *Saccharomyces cerevisiae* S288C: a useful set of strains and plasmids for PCR-mediated gene disruption and other applications. Yeast *14*, 115–132.

Chelstowska, A., and Butow, R.A. (1995). *RTG* genes in yeast that function in communication between mitochondria and the nucleus are also required for expression of genes encoding peroxisomal proteins. J. Biol. Chem. *270*, 18141–18146.

Cherry, J.M., Adler, C., Ball, C., Chervitz, S.A., Dwight, S.S., Hester, E.T., Jia, Y., Juvik, G., Roe, T., Schroeder, M., Weng, S., and Botstein, D. (1998). SGD: *Saccharomyces* genome database. Nucleic Acids Res. *26*, 73–79.

Cortopassi, G.A., and Wong, A. (1999). Mitochondria in organismal aging and degeneration. Biochim. Biophys. Acta *1410*, 183–193.

Costanzo, M.C., Hogan, J.D., Cusick, M.E., Davis, B.P., Fancher, A.M., Hodges, P.E., Kondu, P., Lengieza, C., Lew-Smith, J.E., Lingner, C., Roberg-Perez, K.J., Tillberg, M., Brooks, J.E., and Garrels, J.I. (2000). The yeast proteome database (YPD) and *Caenorhabditis elegans* proteome database (WormPD): comprehensive resources for the organization and comparison of model organism protein information. Nucleic Acids Res. *28*, 73–76.

DeRisi, J.L., Iyer, V.R., and Brown, P.O. (1997). Exploring the metabolic and genetic control of gene expression on a genomic scale. Science *278*, 680–686.

Eisen, M.B., Spellman, P.T., Brown, P.O., and Botstein, D. (1998). Cluster analysis and display of genome-wide expression patterns. Proc. Natl. Acad. Sci. USA *95*, 14863–14868.

Epstein, C.B., Hale, W, IV, and Butow, R.A. (2000). Numerical methods for handling uncertainty in microarray data: an example analyzing perturbed mitochondrial function in yeast. Methods Cell Biol. *66* (in press).

Green, D.R., and Reed, J.C. (1998). Mitochondria and apoptosis. Science *281*, 1309–1312.

Heddi, A., Stepien, G., Benke, P.J., and Wallace, D.C. (1999). Coordinate induction of energy gene expression in tissues of mitochondrial disease patients. J. Biol. Chem. *274*, 22968–22976.

Horswill, A.R., and Escalante-Semerena, J.C. (1997). Propionate catabolism in *Salmonella typhimurium* LT2: two divergently transcribed units comprise the prp locus at 8.5 centisomes, prpR encodes a member of the sigma-54 family of activators, and the prpBCDE genes constitute an operon. J. Bacteriol. *179*, 928–940.

Hughes, T.R., Marton, M.J., Jones, A.R., Roberts, C.J., Stoughton, R., Armour, C.D., Bennett, H.A., Coffey, E., Dai, H., He, Y.D., Kidd, M.J., King, A.M., Meyer, M.R., Slade, D., Lum, P.Y., Stepaniants, S.B., Shoemaker, D.D., Gachotte, D., Chakraburtty, K., Simon, J., Bard, M., and Friend, S.H. (2000). Functional discovery via a compendium of expression profiles. Cell *102*, 109–126.

Jia, Y., Rothermel, B., Thornton, J., and Butow, R.A. (1997). A basic helix-loop-helix zipper transcription complex functions in a signaling pathway from mitochondria to the nucleus. Mol. Cell. Biol. *17*, 1110–1117.

Kal, A.J., van Zonneveld, A.J., Benes, V., vandenBerg, M., Koerkamp, M.G., Albermann, K., Strack, N., Ruijter, J.M., Richter, A., Dujon, B., Ansorge, W., and Tabak, H.F. (1999). Dynamics of gene expression revealed by comparison of serial analysis of gene expression transcript profiles from yeast grown on two different carbon sources. Mol. Biol. Cell *10*, 1859–1872.

Kirchman, P.A., Kim, S., Lai, C.Y., and Jazwinski, S.M. (1999). Interorganelle signaling is a determinant of longevity in *Saccharomyces cerevisiae*. Genetics *152*, 179–190.

Kohrer, K., and Domdey, H. (1991). Preparation of high molecular weight RNA. Methods Enzymol. *194*, 398–405.

Kos, W., Kal, A.J., Vanwilpe, S., and Tabak, H.F. (1995). Expression of genes encoding peroxisomal proteins in *Saccharomyces cerevisiae* is regulated by different circuits of transcriptional control. Biochim. Biophys. Acta *1264*, 79–86.

Kunau, W.-H., Bühne, A.,. Moreno del la Garza, M., Kionka, M., Mateblowski, M., Shultz-Borchard, U., and Thieringer, R. (1988). Comparative enzymology of β-oxidation. Biochem. Soc. Trans. *16*, 418–420.

Liao, X., and Butow, R.A. (1993). RTG1 and RTG2: two yeast genes required for a novel path of communication from mitochondria to the nucleus. Cell *72*, 61–71.

Liao, X.S., Small, W.C., Srere, P.A., and Butow, R.A. (1991). Intramitochondrial functions regulate nonmitochondrial citrate synthase (CIT2) expression in *Saccharomyces cerevisiae*. Mol. Cell. Biol. *11*, 38–46.

Liu, Z., and Butow, R.A. (1999). A transcriptional switch in the expression of yeast tricarboxylic acid cycle genes in response to a reduction or loss of respiratory function. Mol. Cell. Biol. *19*, 6720–6728.

Marshall, P.A., Dyer, J.M., Quick, M.E., and Goodman, J.M. (1996). Redox-sensitive homodimerization of Pex11p: a proposed mechanism to regulate peroxisomal division. J. Cell Biol. *135*, 123–137.

Parikh, V.S., Morgan, M.M., Scott, R., Clements, L.S., and Butow, R.A. (1987). The mitochondrial genotype can influence nuclear gene expression in yeast. Science *235*, 576–580.

Pronk, J.T., van der Linden-Beuman, A., Verduyn, C., Scheffers, W.A., and van Dijken, J.P. (1994). Propionate metabolism in *Saccha-*

romyces cerevisiae: implications for the metabolon hypothesis. Microbiology *140*, 717–722.

Rothermel, B.A., Shyjan, A.W., Etheredge, J.L., and Butow, R.A. (1995). Transactivation by Rtg1p, a basic helix-loop-helix protein that functions in communication between mitochondria and the nucleus in yeast. J. Biol. Chem. *49*, 29476–29482.

Sekito, T., Thornton, J., and Butow, R.A. (2000). Mitochondria-to-nuclear signaling is regulated by the subcellular localization of the transcription factors Rtg1p and Rtg3p. Mol. Biol. Cell *11*, 2103–2115.

Skoneczny, S., Chelstowska, A., and Rytka, A. (1988). Study of the coinduction by fatty acids of catalse A and acyl CoA oxidase in standard and mutant *S. cerevisiae* strains. Eur. J. Biochem. *174*, 297–302.

Tabuchii, T., Serizawa, N., and Uchiyama, H. (1974). A novel pathway for the partial oxidation of propionyl-CoA to pyruvate via seven-carbon tricarboxylic acids in yeasts. Agric. Biol. Chem. *38*, 2571–2572.

Textor, S., Wendisch, V.F., De Graaf, A.A., Muller, U., Linder, M.I., Linder, D., and Buckel, W. (1997). Propionate oxidation in *Escherichia coli*: evidence for operation of a methylcitrate cycle in bacteria. Arch. Microbiol. *168*, 428–436.

van den Berg, M.A., de Jong-Gubbels, P., Kortland, C.J., van Dijken, J.P., Pronk, J.T., and Steensma, H.Y. (1996). The two acetyl-coenzyme A synthetases of *Saccharomyces cerevisiae* differ with respect to kinetic properties and transcriptional regulation. J. Biol. Chem. *271*, 28953–28959.

van Roermund, C.W., Hettema, E.H., van den Berg, M., Tabak, H.F., and Wanders, R.J. (1999). Molecular characterization of carnitine-dependent transport of acetyl-CoA from peroxisomes to mitochondria in *Saccharomyces cerevisiae* and identification of a plasma membrane carnitine transporter, Agp2p. EMBO J. *18*, 5843–5852.

Vanderleij, I., Franse, M.M., Elgersma, Y., Distel, B., and Tabak, H.F. (1993). PAS10 is a tetratricopeptide-repeat protein that is essential for the import of most matrix proteins into peroxisomes of *Saccharomyces cerevisiae*. Proc. Natl. Acad. Sci. USA *90*, 11782–11786.

Veenhuis, M., Mateblowski, M., Kunau, W., and Harder, W. (1987). Proliferation of microbodies in *Saccharomyces cerevisiae*. Yeast *3*, 77–84.

Verduyn, C., Postma, E., Scheffers, W.A., and van Dijken, J.P. (1990). Energetics of *Saccharomyces cerevisiae* in anaerobic glucose-limited chemostat cultures. J. Gen. Microbiol. *136*, 405–412.

Waddle, J.A., Karpova, T.S., Waterston, R.H., and Cooper, J.A. (1996). J. Cell Biol., *132*, 861–870.

Wallace, D.C. (1999). Mitochondrial diseases in man and mouse. Science *283*, 1482–1488.

Wang, S.S., and Brandriss, M.C. (1987). Proline utilization in *Saccharomyces cerevisiae*: sequence, regulation, and mitochondrial localization of the *PUT1* gene product. Mol. Cell. Biol. *7*, 4431–4440.